Electronic supplementary information (ESI)

Conversion of syngas into light olefins over the bifunctional ZnCeZrO/SAPO-34 catalysts: Regulation of the surface oxygen vacancy concentration and its relation to the catalytic performance

Yaoya Luo,[a,b] Sen Wang,*[,a] Shujia Guo,[a,b] Kai Yuan,[a,b] Hao Wang,[a] Mei Dong,[a] Zhangfeng Qin,*[,a] Weibin Fan,[a] Jianguo Wang*[,b]

[a] *State Key Laboratory of Coal Conversion, Institute of Coal Chemistry, Chinese Academy of Sciences, P.O. Box 165, Taiyuan, Shanxi 030001, PR China*

[b] *University of the Chinese Academy of Sciences, Beijing 100049, PR China*

[*] *Corresponding authors. Tel.: +86-351-4046092; Fax: +86-351-4041153. E-mail address: qzhf@sxicc.ac.cn (Z. Qin); wangsen@sxicc.ac.cn (S. Wang); iccjgw@sxicc.ac.cn (J. Wang)*

As the Electronic supplementary information (ESI) of the manuscript "*Conversion of syngas into light olefins over the bifunctional ZnCeZrO/SAPO-34 catalysts: Regulation of the surface oxygen vacancy concentration and its relation to the catalytic performance*", following materials are provided:

More characterization results for the $Zn_{0.5}CeZrO_x$ composite oxides prepared with different complexing agents and calcined at different temperatures; optimization of the reaction conditions for the conversion of syngas to olefins over the $Zn_{0.5}CeZrO_x$-glucose-500/SAPO-34 bifunctional catalyst.

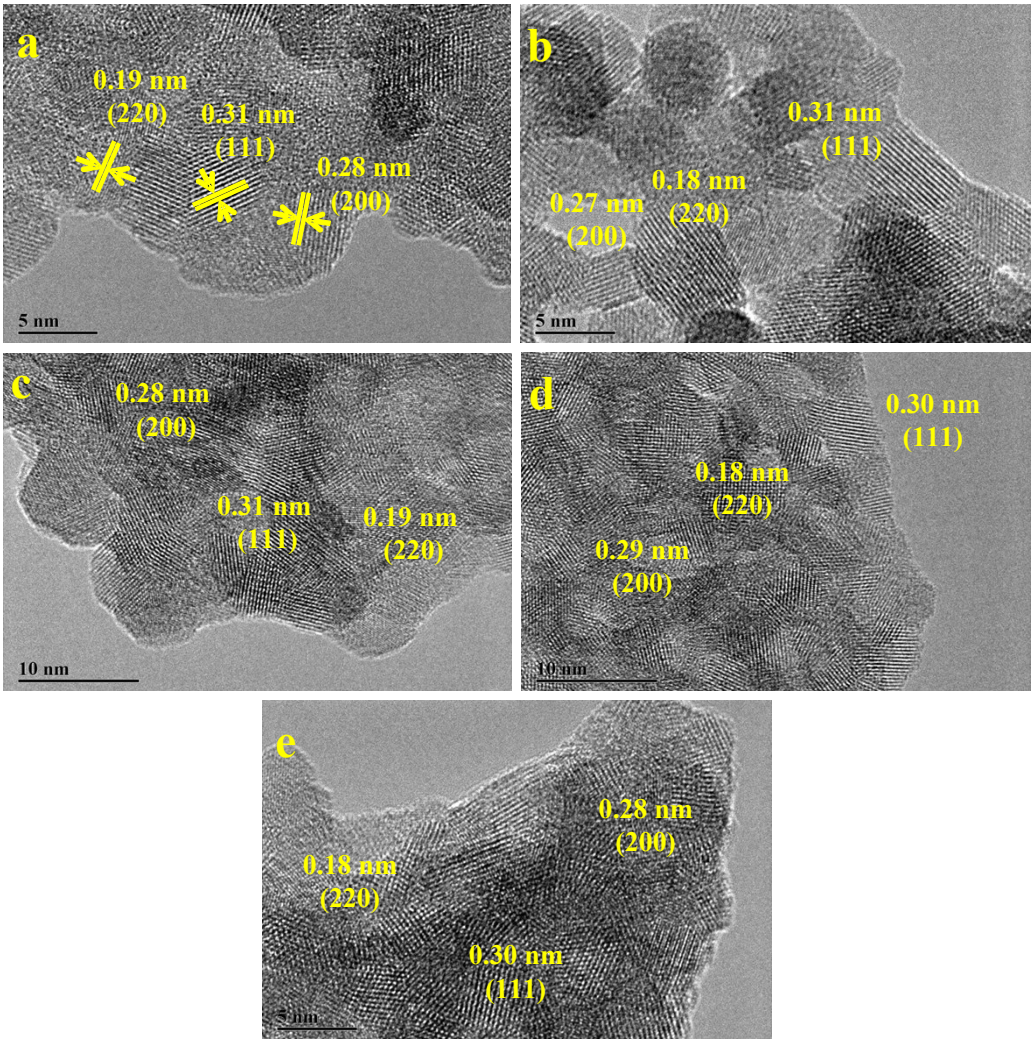

Fig. S1. HR-TEM images of the $Zn_{0.5}CeZrO_x$ composite oxides prepared with different complexing agents: (a) $Zn_{0.5}CeZrO_x$-glucose, (b) $Zn_{0.5}CeZrO_x$-citric acid, (c) $Zn_{0.5}CeZrO_x$-tartaric acid, (d) $Zn_{0.5}CeZrO_x$-adipic acid, and (e) $Zn_{0.5}CeZrO_x$-L-alanine.

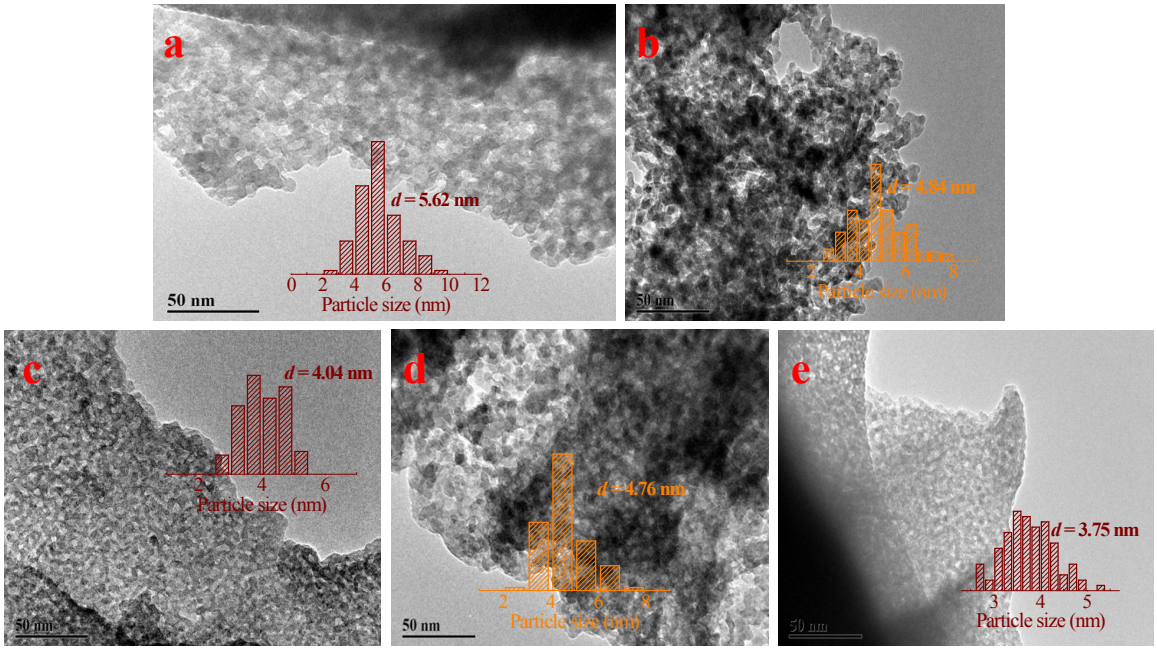

Fig. S2. TEM images and size distributions (estimated by counting more than 100 particles) of the $Zn_{0.5}CeZrO_x$ composite oxides prepared with different complexing agents: (a) $Zn_{0.5}CeZrO_x$-glucose, (b) $Zn_{0.5}CeZrO_x$-citric acid, (c) $Zn_{0.5}CeZrO_x$-tartaric acid, (d) $Zn_{0.5}CeZrO_x$-adipic acid, and (e) $Zn_{0.5}CeZrO_x$-L-alanine.

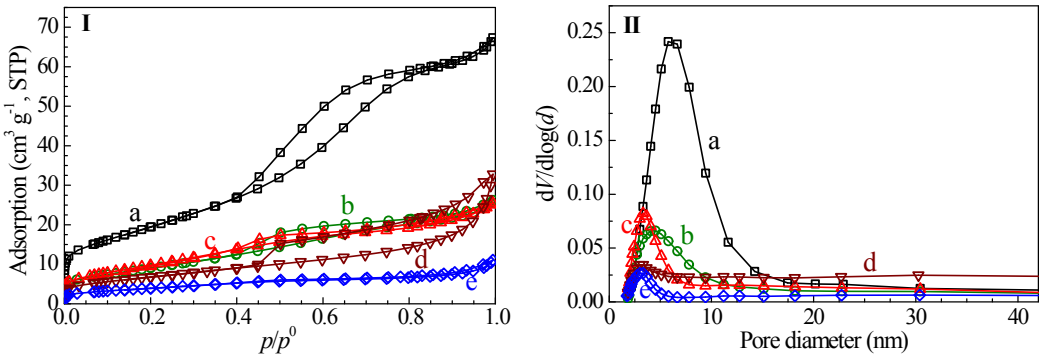

Fig. S3. N_2 adsorption-desorption isotherms **(I)** and corresponding pore size distribution curves **(II)** of the $Zn_{0.5}CeZrO_x$ composite oxides prepared with different complexing agents: (a) $Zn_{0.5}CeZrO_x$-glucose, (b) $Zn_{0.5}CeZrO_x$-citric acid, (c) $Zn_{0.5}CeZrO_x$-tartaric acid, (d) $Zn_{0.5}CeZrO_x$-adipic acid, and (e) $Zn_{0.5}CeZrO_x$-L-alanine.

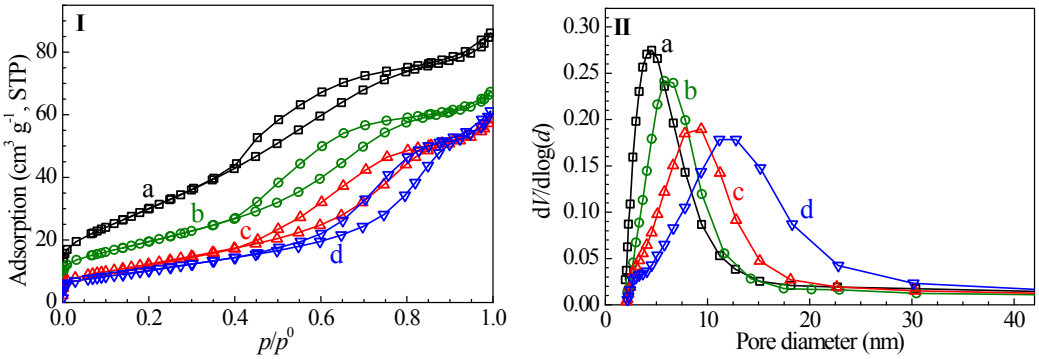

Fig. S4. N_2 absorption-desorption isotherms **(I)** and corresponding pore size distribution curves **(II)** of the $Zn_{0.5}CeZrO_x$-glucose composite oxides (prepared with glucose as the complexing agent) calcined at different temperatures: (a) 400 °C; (b) 500 °C; (c) 600 °C; and (d) 700 °C.

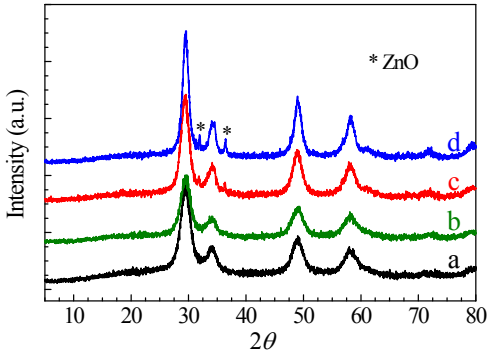

Fig. S5. XRD patterns of the $Zn_{0.5}CeZrO_x$-glucose composite oxides (prepared with glucose as the complexing agent) calcined at different temperatures: (a) 400 °C; (b) 500 °C; (c) 600 °C; and (d) 700 °C.

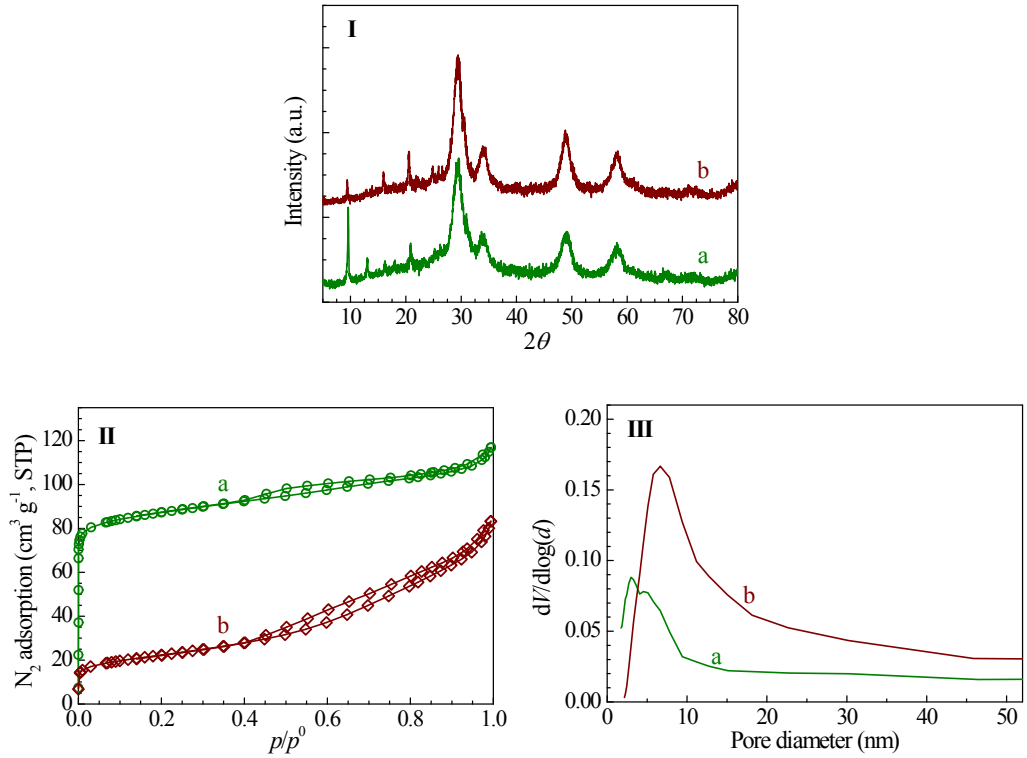

Fig. S6. XRD patterns **(I)**, N_2 adsorption-desorption isotherms **(II)** and corresponding pore size distribution curves **(III)** of the $Zn_{0.5}CeZrO_x$-glucose/SAPO-34 composite catalyst before (a, fresh) and after enduring the reaction of syngas to light olefins (b, spent).

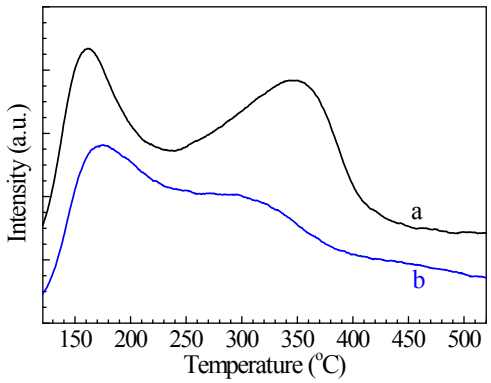

Fig. S7. NH_3-TPD profiles of the SAPO-34 molecular sieve (a) and the $Zn_{0.5}CeZrO_x$-glucose/SAPO-34 composite catalyst (b).

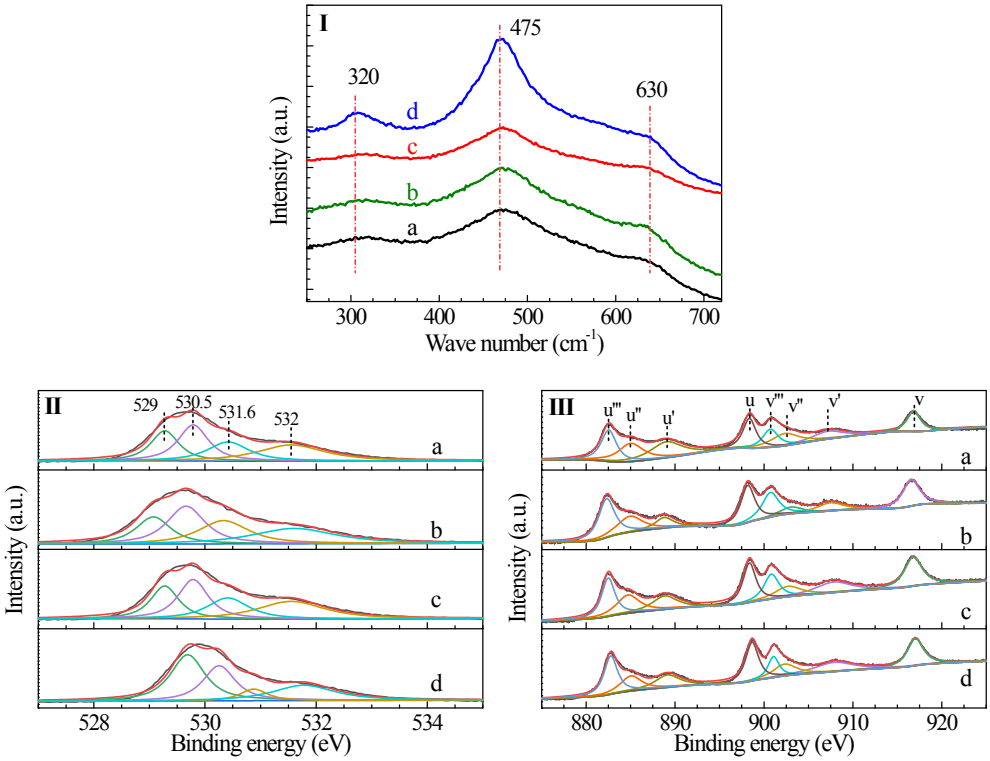

Fig. S8. Raman spectra **(I)**, O(1s) XPS spectra **(II)**, and Ce(3d) XPS spectra **(III)** of the $Zn_{0.5}CeZrO_x$-glucose composite oxides (prepared with glucose as the complexing agent) calcined at different temperatures: (a) 400 °C; (b) 500 °C; (c) 600 °C; and (d) 700 °C.

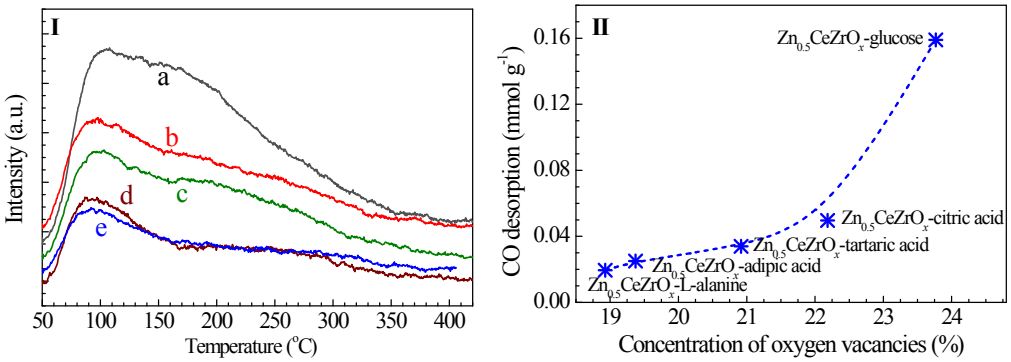

Fig. S9. (I) CO-TPD profiles of the $Zn_{0.5}CeZrO_x$ composite oxides prepared with different complexing agents: (a) $Zn_{0.5}CeZrO_x$-glucose, (b) $Zn_{0.5}CeZrO_x$-citric acid, (c) $Zn_{0.5}CeZrO_x$-tartaric acid, (d) $Zn_{0.5}CeZrO_x$-adipic acid, and (e) $Zn_{0.5}CeZrO_x$-L-alanine. **(II)** Variation of the CO adsorption quantity obtained from CO-TPD with the concentration of surface oxygen vacancies of the $Zn_{0.5}CeZrO_x$ composite oxides measured by O 1s XPS. The desorption amount of CO was calculated according to the peak area between 150 and 350 °C in the CO-TPD profiles; as the desorption of CO on the ZnCeZrO composite oxide appears in general at 50–320 °C and levels off with the temperature above 350 °C, the recording of the CO-TPD profiles of several samples ends at 450–500 °C.

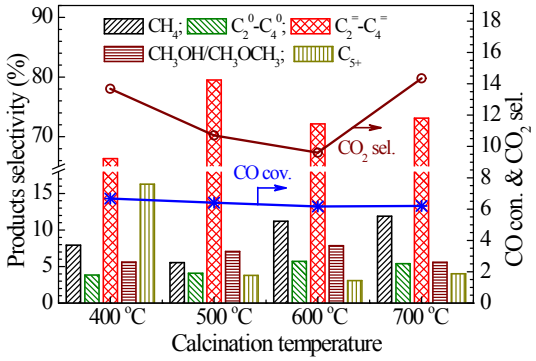

Fig. S10. CO conversion and products selectivity for the conversion of syngas over the $Zn_{0.5}CeZrO_x$-glucose/SAPO-34 bifunctional catalysts calcined at different temperatures (400, 500, 600 and 700 °C). Reaction conditions: H_2/CO = 2/1, 300 °C, 1.0 MPa, GHSV = 5400 mL/g·h, 30 h, $Zn_{0.5}CeZrO_x$/SAPO-34 = 1 (by mass); reported at a TOS of 30 h.

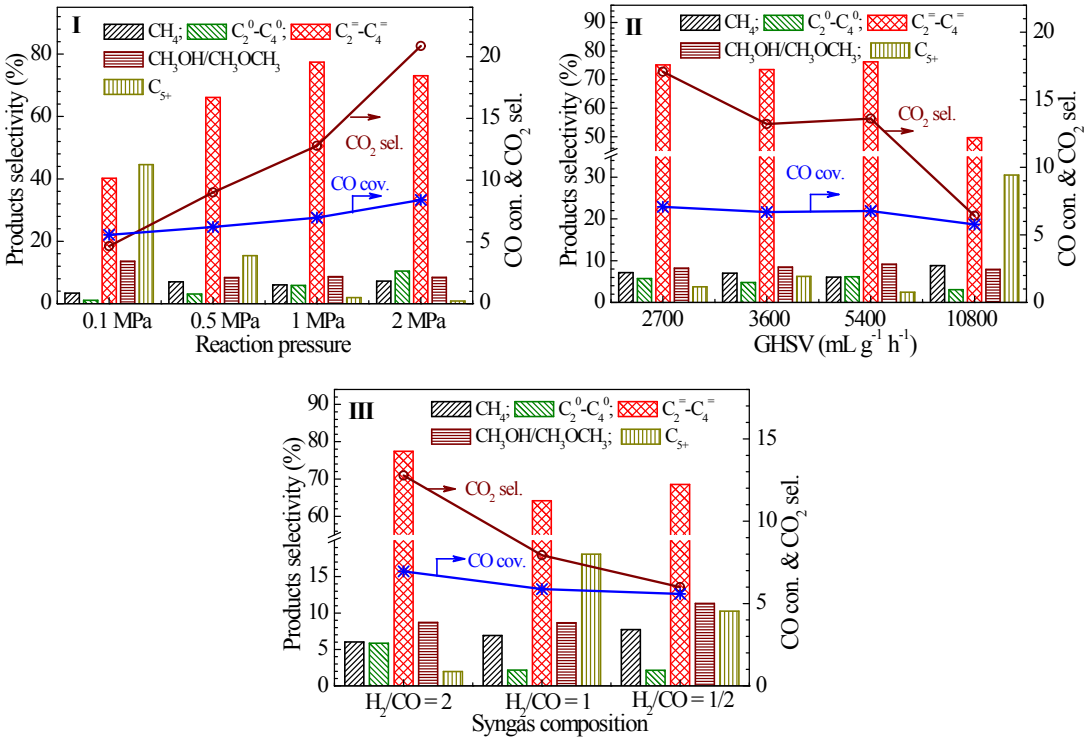

Fig. S11. Influences of the reaction pressure **(I)**, gas hourly space velocity **(II)**, and syngas H_2/CO ratio **(III)** on the CO conversion and products distribution for the conversion of syngas over the $Zn_{0.5}CeZrO_x$-glucose-500/SAPO-34 bifunctional catalyst. Except that specified at the graph abscissa, the reaction was carried out under a H_2/CO molar ratio of 2, 300 °C, 1.0 MPa, GHSV = 5400 mL g^{-1} h^{-1}, $Zn_{0.5}CeZrO_x$/SAPO-34 = 1 (by mass); the data were reported at a TOS of 15 h.